J. Fluid Mech. (2002), *vol.* 469, *pp.* 237–256.
DOI: 10.1017/S0022112002001714 Printed in the United Kingdom

Viscous fingering in non-Newtonian fluids

By ANKE LINDNER[1]†, DANIEL BONN[1], EUGENIA CORVERA POIRÉ[2], MARTINE BEN AMAR[1] AND JACQUES MEUNIER[1]

[1]Laboratoire de Physique Statistique, Ecole Normale Supérieure, 24 Rue Lhomond, 75231 Paris Cedex 05, France

[2]Departamento de Física y Química Teórica, Facultad de Química, UNAM, Ciudad Universitaria, México, DF 04510, México

(Received 21 February 2001 and in revised form 13 May 2002)

We study the viscous fingering or Saffman–Taylor instability in two different dilute or semi-dilute polymer solutions. The different solutions exhibit only one non-Newtonian property, in the sense that other non-Newtonian effects can be neglected. The viscosity of solutions of stiff polymers has a strong shear rate dependence. Relative to Newtonian fluids, narrower fingers are found for rigid polymers. For solutions of flexible polymers, elastic effects such as normal stresses are dominant, whereas the shear viscosity is almost constant. Wider fingers are found in this case. We characterize the non-Newtonian flow properties of these polymer solutions completely, allowing for separate and quantitative investigation of the influence of the two most common non-Newtonian properties on the Saffman–Taylor instability. The effects of the non-Newtonian flow properties on the instability can in all cases be understood quantitatively by redefining the control parameter of the instability.

1. Introduction

Viscous fingering has received much attention as an archetype of pattern-forming systems and as a limiting factor in the recovery of crude oil (Saffman & Taylor 1958; for reviews see Bensimon *et al.* 1986; Homsy 1987; Couder 1991). Viscous fingers form when in a thin linear channel or Hele-Shaw cell, a fluid pushes a more viscous fluid. The interface between the fluids develops an instability leading to the formation of finger-like patterns. The viscous fingering instability has been studied intensively over the past few decades, both theoretically and experimentally. Compared to other pattern-formation problems, this is likely to be due to its relative simplicity. Indeed, the mathematically interesting structure of the governing equations is also at the root of much of the theoretical interest; the problem is typical of many Laplacian free-boundary problems (Couder 1991). Although highly nonlinear, the problem has been solved numerically; for some limiting cases, analytical results have been obtained.

A whole different class of problems was uncovered somewhat later, when the instability was studied for non-Newtonian fluids. For these, strikingly different

† Present address: Laboratoire de Physico-Chimie Structurale et Macromoléculaire, Ecole Supérieure de Physique et de Chimie Industrielles, 10, rue Vauquelin, 75231 Paris Cedex 05, France.

fingering patterns are found (Daccord, Nittmann & Stanley 1986; Lemaire *et al.* 1991; McCloud & Maher 1995; Bonn, Kellay & Meunier 1998). Experiments in, for instance, foams, clay pastes, slurries and polymer gels reveal branched fractal or fracture-like patterns (van Damme *et al.* 1988; Zhao & Maher 1993; Park & Durian 1994). The physical origin of the very different structures is so far ill understood, mainly also because the visco-elastic characteristics of most of these fluids were not determined simultaneously. Recently, a number of experiments have been performed in somewhat simpler systems: dilute or semidilute polymer solutions (Smith *et al.* 1992; Bonn *et al.* 1995; Bonn & Meunier 1997; Kawaguchi *et al.* 1998). In these experiments, both a narrowing (Smith *et al.* 1992; Bonn & Meunier 1997), and a widening (Bonn *et al.* 1995) of the fingers with respect to the Newtonian case was reported upon addition of small amounts of polymers in the driven fluid.

The main mathematical challenge the 'visco-elastic fingering' instability poses is that the pressure field may no longer be Laplacian, making even a numerical prediction of the finger width difficult, but in some cases not impossible (Kondic, Palffy-Muhoray & Shelley 1998; Ben Amar & Corvera Poiré 1999). Detailed theory on the visco-elastic fingering instability has attempted to account for some of these features, mainly focusing on shear-thinning behaviour (Wilson 1990; Sader, Chan & Hughes 1994; Ben Amar 1995; Bonn *et al.* 1995; Kondic *et al.* 1996, 1998; Corvera Poiré & Ben Amar 1998; Ben Amar & Corvera Poiré 1999; Fast *et al.* 2001). Some authors also attempt to take other non-Newtonian effects, such as normal stresses into account (Wilson 1990; Ro & Homsy 1995). Other authors have analysed a Maxwell fluid in a tube and derived a dynamic generalization of Darcy's law in the frequency domain (del Río, López de Haro & Whitaker 1998).

Most of the fluids studied in the experiments, on the other hand, exhibit a number of different non-Newtonian properties. Notably, polymer solutions can exhibit both shear thinning and normal stress effects, which have been shown to lead to opposite effects (finger narrowing and finger widening) on the instability (Bonn *et al.* 1995; Bonn & Meunier 1997). Additionally, the viscous fingering instabilities in, for instance, pastes or gels are more difficult to understand since these fluids have a yield stress, show shear thinning, and possibly have other elastic effects also.

Here, we attempt to disentangle the influence that different non-Newtonian flow properties have on the instability. To do so, we study fingering in two different dilute or semi-dilute polymer solutions, that each exhibit only one non-Newtonian property, in the sense that other non-Newtonian effects can be neglected. For solutions of flexible polymers, elastic effects such as normal stresses and a large elongational viscosity are dominant, whereas the shear viscosity is almost constant. Stiff polymers, on the other hand, may show a strong dependence of the viscosity on the shear rate, but almost negligible elastic effects (i.e. normal stresses). We characterize the non-Newtonian flow properties of these polymer solutions completely, allowing for separate and quantitative investigation of the influence of the two most common non-Newtonian properties on the Saffman–Taylor instability: shear thinning and normal stress effects. Probably the third most common non-Newtonian property is a yield stress; we previously studied the effect of a yield stress on the instability (Lindner, Coussot & Bonn 2000*a*). This paper is organized as follows. In § 2, we will recall the basic equations for the Saffman–Taylor instability and § 3 deals with the systems and experimental methods. In §§ 4 and 5, we will treat the effect of shear-thinning and normal stresses on the instability, respectively; the results are summarized in § 6.

2. The Saffman–Taylor instability

For Newtonian fluids, the motion of a fluid between the two horizontally spaced plates of the Hele-Shaw cell is described by the two-dimensional velocity field v averaged through the thickness of the cell. It is given by Darcy's law, which relates the local pressure gradient to the fluid velocity v as:

$$v = -\frac{b^2}{12\mu}\nabla p, \tag{1}$$

where b is the plate spacing of the Hele-Shaw cell and μ is the shear viscosity. It follows immediately that, if the fluid is incompressible, the pressure field satisfies Laplace's equation:

$$\Delta p = 0. \tag{2}$$

If the fluid is displaced by another, less viscous, fluid, the interface between the two fluids is unstable, and viscous fingers will form. In the experiments, we use air as the driving fluid; we can neglect its viscosity. Therefore, Darcy's law applies for the driven fluid with viscosity μ. The pressure field is also calculated within the driven fluid with, in addition, a pressure jump over the interface owing to the surface tension:

$$\delta p = \sigma/R, \tag{3}$$

with σ the interfacial tension and R the radius of curvature of the interface, again employing a two-dimensional approximation, as was justified in the limit of small capillary number by Park & Homsy (1984), and Reinelt & Saffman (1985). The other boundary conditions are the continuity condition, which implies that the normal velocity at both sides of the interface is equal and a far-field value for the pressure. Supplemented with these boundary conditions, equations (1)–(3) constitute the complete set of equations that must be solved in order to obtain the finger shape.

For characterizing the instability quantitatively, most studies have focused on the width of the finger w relative to the channel width W, $\lambda = w/W$ as a function of their velocity. It follows from the above that their width is determined by the capillary number $Ca = \mu U/\sigma$, which represents the ratio of viscous forces $\mu U/R$ and capillary forces σ/R. The finger velocity U is related to the velocity v of the fluid far from the finger by mass conservation, $U = \lambda v$. The viscous forces tend to narrow the finger, whereas the capillary forces tend to widen it. We thus anticipate that the relative width of the viscous fingers decreases with increasing finger velocity. This is indeed what is observed experimentally; however, for very large values of the capillary parameter, λ does not go to zero but reaches a limiting value of about half the channel width.

The control parameter for the fingering problem is $1/B = 12Ca(W/b)^2$ with W/b again the aspect ratio of the Hele-Shaw cell. When scaled on $1/B$, measurements of λ for different systems all fall on the same universal curve. In the ideal, Newtonian, two-dimensional situation $1/B$ is consequently the only parameter that selects the finger width.

In the absence of surface tension, Saffman & Taylor (1958) found a family of analytical solutions of the shape of the interface in Cartesian coordinates $x(y)$ given by:

$$x = \frac{W(1-\lambda)}{2\pi}\ln\left[\frac{1}{2}\left(1+\cos\frac{2\pi y}{\lambda W}\right)\right]. \tag{4}$$

The form of the finger obtained from (4) for $\lambda = 0.5$ (where the surface tension is least important) agrees well with the experimentally observed finger shapes.

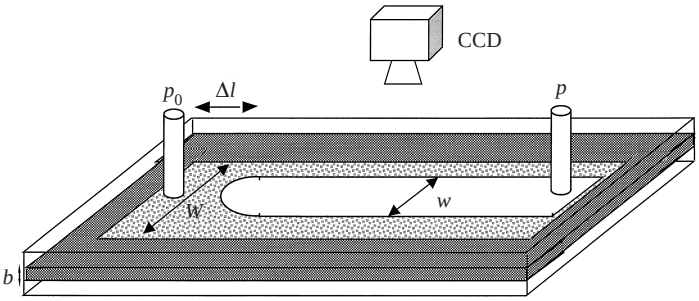

FIGURE 1. Schematic drawing of the experimental set-up.

However, (4) does not explain the finger selection, i.e. it does not relate λ to $1/B$. In order to account for that, the surface tension has to be taken into account. This was done numerically by McLean & Saffman (1981) who determined the dependence of the universal curve for λ on $1/B$. Their results were found to agree well with the experimental determinations. Only much later was the selection problem solved analytically (Shraiman 1986; Hong & Langer 1986; Combescot *et al.* 1986).

3. Experimental

The rheology of the polymer solutions was studied on a Reologica Stress-Tech (cone-plate geometry) rheometer equipped with a normal force transducer. We use a large cone (55 mm) with a small angle (0.5°) in order to detect small normal stress differences at high shear rates.

The viscous fingering experiments are performed for the polymer solutions in a rectangular Hele-Shaw cell consisting of two glass plates separated by a thin Mylar spacer, fixing the plate spacing b which can be changed from $b = 0.25$ mm to $b = 1$ mm. Three different channel widths are used: $W = 2$, 4 and 8 cm. We constructed a long Hele-Shaw cell (> 1 m) for this study in order to verify that we are indeed in a steady state and the finger does not change in time. This was the case for all the experiments reported here. The cell is filled with the polymer solution, and compressed air is used as the less viscous driving fluid. The design of the experimental cell is shown figure 1. The fingers are captured by a CCD camera coupled to a VCR. This allows for measurements of the width w as a function of the velocity U of the tip of the finger.

Furthermore, we measure the pressure at the inlet and outlet of the cell either by a pressure transducer or a water column manometer in order to obtain the applied pressure gradient.

For the experiments on rigid polymers described below, we use solutions of xanthane, a stiff rodlike polysaccharide with an average molecular weight of $M_w = 3 \times 10^6\,\mathrm{g\,mol^{-1}}$, obtained from Aldrich. Rheological measurements show that the overlap concentration c^* is 50 w.p.p.m. (parts per million per weight), so that the measurements presented below are in the dilute and semi-dilute regime. The surface tension σ for the air/xanthane solution is $72 \pm 2\,\mathrm{mN\,m^{-1}}$ (Lindner, Bonn & Meunier 2000*b*), independent of polymer concentration over the range of concentrations used in our experiments and thus very close to the surface tension of pure water ($72.3\,\mathrm{mN\,m^{-1}}$).

For the experiments on flexible polymers we use polyethylene oxide (PEO) grade WSR301 from Union Carbide; its molecular weight $M_w = 4 \times 10^6$ is close to that of

the xanthane. Rheological measurements show that the overlap concentration c^* is 400 w.p.p.m., so that the measurements presented below are in the dilute and semi-dilute regime. The surface tension σ for the air/PEO solution is $63 \pm 2\,\mathrm{mN\,m^{-1}}$ (Bonn & Meunier 1997), and is again found to be independent of polymer concentration over the range of concentrations used in our experiments. The slight lowering of the surface tension with respect to that of pure water indicates that some adsorption (either of the polymer or of some impurities) takes place at the air/solution interface.

4. Effect of shear-thinning: the rigid polymer xanthane

4.1. *Rheology and Darcy's law*

To characterize the solutions of xanthane, the viscosity and the normal stress difference were determined previously for a range of shear rates from $10 < \dot{\gamma} < 1000\,\mathrm{s^{-1}}$, corresponding to the range of shear rates typically encountered in the viscous fingering experiments (Lindner *et al.* 2000*b*). It was concluded that, for low concentrations, the viscosity depends only slightly on the shear rate and thus deviations from Newtonian behaviour are small. With increasing polymer concentration, the viscosity decreases more strongly with increasing shear rate and strong deviations from Newtonian behaviour are found. Xanthane solutions are shear thinning, and it was found that a satisfactory description of most of the data can be obtained using the Ostwald–de Waele power law model (Bird, Armstrong & Hassager 1987) for the viscosity μ, $\mu = k_1 \dot{\gamma}^{(n-1)}$ (with $1 > n > 0$). The viscosity shows a power law dependence on the shear rate. The values for n and k_1 for the polymer solutions used in the following can be found in Lindner *et al.* (2000*b*). Note that the obtained power n is a measure for the shear thinning character of the fluid; $n = 1$ corresponds to a Newtonian fluid, and the solutions become more shear thinning as n decreases. For the whole concentration range studied here ($0 < c < 2000$ w.p.p.m.) no measurable normal stresses were found in the range of shear rates studied ($10 < \dot{\gamma} < 6000\,\mathrm{s^{-1}}$); the uncertainty on the measurements is of the order of 10 Pa. Estimates for the shear rates present in the system (given in more detail below) show that it is unlikely that much higher shear rates than these are present. The dominant non-Newtonian character of the solutions of xanthane in shear flow for the concentration and shear range under study is therefore the shear thinning character of the viscosity.

In addition, Lindner *et al.* (2000*b*) studied Darcy's law, equation (1), directly in the Hele-Shaw cell. They compared the experimentally obtained relation between $v = \lambda U$ and ∇p to the rheology data. The average shear rate in the Hele-Shaw cell can be obtained as the average velocity gradient by supposing the flow profile remains parabolic, $\dot{\gamma} = 3U/b$ to a first approximation. It was found that predictions of Darcy's law in which the viscosity is simply replaced by the shear-thinning viscosity remains valid for low concentrations (50 w.p.p.m., 100 w.p.p.m.) corresponding to weak shear thinning. For higher concentrations (500 w.p.p.m., 1000 w.p.p.m.) and thus strong shear thinning, Darcy's law has to be modified further, taking into account the modification of the parabolic flow profile. If this is done, again, good agreement is obtained between the rheology data and the measurements in the Hele-Shaw cell (Lindner *et al.* 2000*b*).

4.2. *Finger selection*

4.2.1. *Weak shear thinning: low polymer concentration*

We previously measured (Lindner *et al.* 2000*b*) the finger width w as a function of the finger tip velocity U for solutions of xanthane at different concentrations of

50–1750 w.p.p.m. To be able to compare the experimental results with the theoretical predictions of McLean & Saffman (1981) for Newtonian fluids, the curves for λ were scaled on a modified control parameter $1/B$. For this, the shear thinning character of the fluids is taken into account by replacing μ by the shear dependent viscosity $\mu(\dot{\gamma})$ (van Damme *et al.* 1988; Lindner *et al.* 2000*b*). We found that for low polymer concentrations (weak shear thinning) the finger width as a function of $1/B$ falls on the universal curve for Newtonian fluids. For increasing polymer concentration, the results for the finger width start to deviate from the universal curve. For high polymer concentration and large $1/B$, the finger width is found to be smaller than the classical limit. To distinguish between the two regimes, it is worth noting that the results for λ start to deviate from the universal curve for Newtonian fluids for concentrations similar to those where we also observed deviations from the modified Darcy's law (Lindner *et al.* 2000*b*).

4.2.2. *Strong shear thinning: high polymer concentration*

For higher polymer concentrations, we observed fingers that are significantly narrower than the classical limit for Newtonian fluids (Bonn & Meunier 1997; Lindner *et al.* 2000*b*). A snapshot of such a finger is shown in figure 2(*a*). Fingers of width less than $\lambda = 0.5$ have also been observed in Newtonian fluids, when the finger is disturbed by the presence of an anisotropy in the system. The anisotropy can, for example, be caused by placing a bubble in front of the finger tip (Couder *et al.* 1986; Rabaud, Couder & Gerard 1988), by engraving the middle of the glass plates of the Hele-Shaw cell in the direction of the finger propagation (Rabaud *et al.* 1988), or by a thread stretched along the cell (Zocchi *et al.* 1987; Rabaud *et al.* 1988). Such a perturbation of the finger systematically destroys the classical limit of $\lambda = 0.5$ for high velocities, independently of the exact nature of the perturbation. If the perturbation introduces an anisotropy facilitating flow in the direction of the finger growth, we observe the formation of fingers with a relative finger width $\lambda < 0.5$ that tend toward zero for high velocities. Similar behaviour is also found in theoretical studies in which the perturbation is incorporated in an anisotropic surface tension (Shaw 1980; Kessler & Levine 1985). A similar effect might occur also at the origin of the finger narrowing for the polymer solutions; the shear dependent viscosity can be understood as an anisotropy of the system. Regions of high fluid velocity corresponding to a high shear rate should have a small viscosity due to the shear-thinning character of the polymer solution. This is essentially the case in front of the finger tip, as is confirmed by the numerical simulations of Kondic *et al.* (1998) and Fast *et al.* (2001); this anisotropy leads to a preferred growth direction in the direction of movement of the finger.

To obtain more information about the selection mechanism for strong shear thinning, we vary the cell geometry from $W = 2\,\mathrm{cm}$ to $W = 8\,\mathrm{cm}$ and from $b = 0.25\,\mathrm{mm}$ to $b = 1\,\mathrm{mm}$. In figure 3, we depict the results for λ as a function of the velocity for a 1000 w.p.p.m. solution and three different widths of the cell. It can be observed that the relative finger width decreases with increasing channel width and does not stabilize on a unique plateau value at high velocities for the different geometries. For Newtonian fluids, variations of λ with the channel width are observed only for low velocities. For high velocities, the relative finger width stabilizes on a plateau value of $\lambda = 0.5$, independently of the channel width. The conclusion must therefore be that the selection mechanism of the shear thinning fingers is entirely different from that for Newtonian fluids.

Our results are in fact similar to observations made by Rabaud *et al.* (1988) for Newtonian fluids, but with engraved glass plates of the Hele-Shaw cell. They

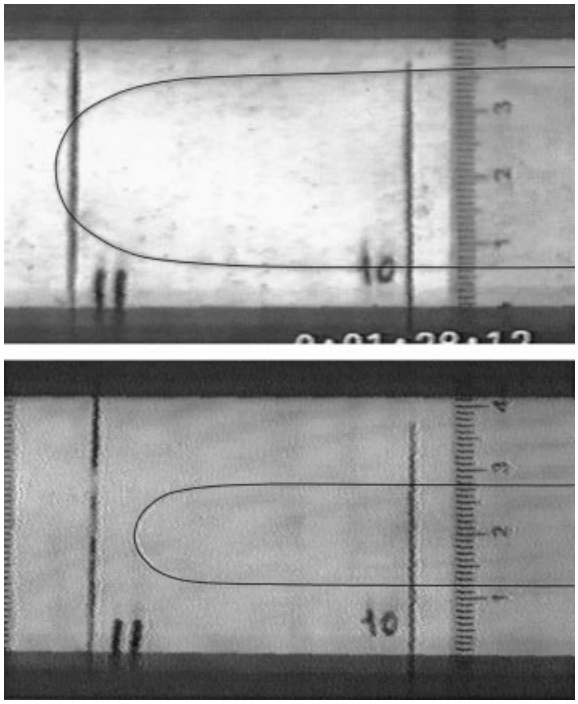

FIGURE 2. Snapshots of a finger for (*a*) a solution of 50 w.p.p.m. of PEO, and (*b*) a solution of 1000 w.p.p.m. of xanthane at high velocity (4 cm s^{-1}) for a channel with $W = 4$ cm and $b = 0.25$ mm.

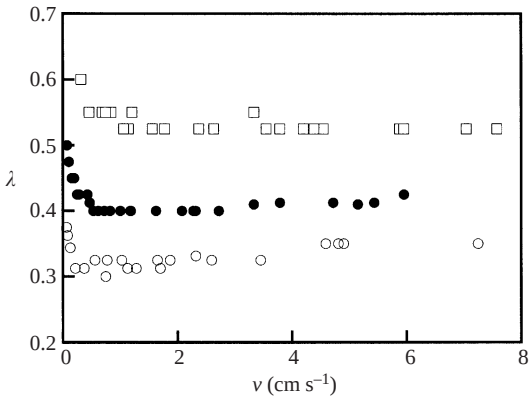

FIGURE 3. Results for λ as a function of the velocity for a 1000 w.p.p.m. xanthane solution and three different widths of the cell. □, 2 cm; ●, 4 cm; ○, 8 cm.

also found 'anomalous' viscous fingers with a finger width significantly smaller than $\lambda = 0.5$ at high velocities. This observation is explained by the fact that engravings represent a local perturbation at the finger tip. This disturbance removes the selection of the discrete set of solutions (with $\lambda = 0.5$ at high velocities) found normally. The continuum of solutions given by the analytical result of Saffman & Taylor without surface tension, equation (4), then becomes possible; λ can take values smaller than $\lambda = 0.5$ at high velocity. Rabaud *et al.* (1988) indeed show that the form of the narrow fingers is well described by equation (4).

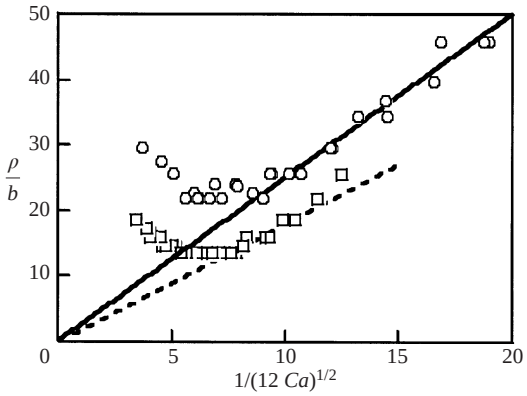

FIGURE 4. Dimensionless radius of curvature as a function of the inverse square root of the capillary number for ○, 500 and □, 1000 w.p.p.m. xanthane solutions for a channel with $W = 4$ cm and $b = 0.25$ mm.

Rabaud *et al.* show that for a given value of capillary number, it is the dimensionless radius of curvature at the tip ρ/b that is selected. As a direct consequence, for a given velocity, the anomalous fingers obtained in cells of different aspect ratios have different widths, as was also observed for the shear thinning fluid (figure 3). More quantitatively, Rabaud *et al.* obtain ρ from the observed λ, by expanding the tip radius from equation (4) for small λ to find:

$$\rho = \frac{\lambda^2 W}{\pi(1-\lambda)}, \tag{5}$$

a result that becomes exact as $\lambda \to 0$. Their experiments show that the dimensionless radius of curvature ρ/b follows (Rabaud *et al.* 1988)

$$\frac{\rho}{b} = \frac{\alpha}{\sqrt{12Ca}}, \tag{6}$$

where α is a proportionality constant. Equations (5) and (6) yield λ as a function of Ca, and therefore solve the selection problem.

We find that a similar mechanism is also responsible for the selection of the viscous fingers in a shear thinning fluid. We find that the finger shapes agree well with the analytical prediction of Saffman & Taylor, equation (4), provided $\lambda < 0.65$, so that again surface tension effects are small. Subsequently, we can use equation (5) to calculate ρ from the experimental λ, obtaining ρ/b as a function of $1/\sqrt{Ca}$ from the experimental determination of $\lambda(U)$. The viscosity μ is, as before, substituted by the shear dependent viscosity $\mu(\dot{\gamma})$. The results for 500 w.p.p.m. and 1000 w.p.p.m. are shown in figure 4 for a channel with $W = 4$ cm and $b = 0.25$ mm. We observe a region where the relation between ρ/b and $1/\sqrt{Ca}$ is linear, as for the anomalous fingers (Rabaud *et al.* 1988). For high velocities (corresponding to low $1/\sqrt{Ca}$), we observe a saturation of ρ/b (also observed by Rabaud *et al.* for Newtonian fluids) that we will discuss below.

For the linear part, we find a slope $\alpha = 2.5$ for 500 w.p.p.m. and $\alpha = 1.8$ for 1000 w.p.p.m. Note that the value of α depends on the concentration of the solutions and thus the shear thinning character of the fluids. The relation between α and the shear thinning character of the solutions can be quantified further with the help of the power law model. The results for α as a function of the shear-thinning exponent n for

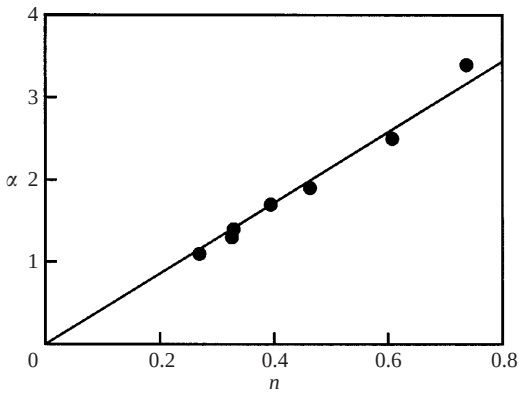

FIGURE 5. Slope α of the plot of figure 3 as a function of the shear-thinning exponent n for different xanthane solutions.

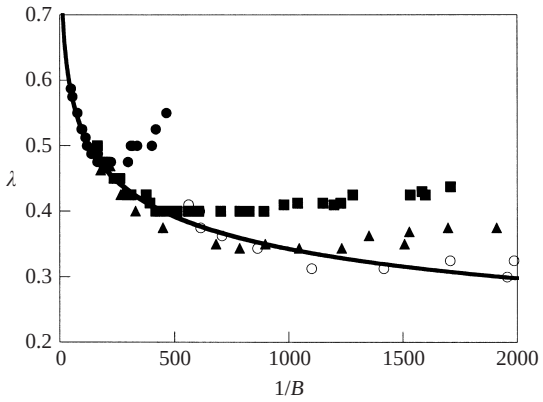

FIGURE 6. Experimental results for the finger width for a concentration of 1000 w.p.p.m. xanthane and different cell geometries. ●, $W = 4$ cm, $b = 0.66$ mm; ■, $W = 4$ cm, $b = 0.25$ mm; ▲, $W = 8$ cm, $b = 0.5$ mm; ○, $W = 8$ cm, $b = 0.25$ mm. The curve $\lambda(1/B)$ from equation (7) is shown as the drawn line.

a concentration range of $c = 250$ w.p.p.m. ($n = 0.73$) to $c = 2000$ w.p.p.m. ($n = 0.33$) are depicted in figure 5, from which we conclude that the relation between α and n is linear, $\alpha = 4.29\,n$.

This again solves the selection problem as it is now possible to obtain the value of α from the power of the shear thinning viscosity, obtained by rheological measurements. To compare the obtained results with the classical results of McLean & Saffman, it is useful to be able to represent λ as a function of $1/B$. From equations (5) and (6), it follows that (Rabaud *et al.* 1988):

$$\lambda = \frac{\pi\alpha\sqrt{B}}{2}\left[\left(1 + \frac{4}{\pi\alpha\sqrt{B}}\right)^{1/2} - 1\right]. \tag{7}$$

With this result, once α is known, we obtain $\lambda(1/B)$. The experimental results before the saturation for a given concentration but different geometries, should all fall on this curve. Figure 6 depicts the experimental results for a concentration of 1000 w.p.p.m. and different cell geometries are shown as well as the curve $\lambda(1/B)$ from equation (7); the experimental results for different geometries fall on one universal

curve given by equation (7), even if the observed finger widths are not very small. We therefore conclude that equation (7) provides a satisfactory description of the data before the saturation occurs.

The only remaining problem is then the saturation observed for the radius of curvature for low values of $1/\sqrt{Ca}$; the experimental results λ as a function of $1/B$ deviate from the universal curve at a given value of $1/B$, that depends on the geometry. In addition, for certain aspect ratios of the Hele-Shaw cell, the saturation even turns into an increase of the finger width with increasing $1/B$.

Although we have no explanation for these observations, especially for the increase of λ with $1/B$, it is worth noting that for the anomalous fingers of Rabaud *et al.* a saturation was also observed. For the latter, the saturation occurs typically when ρ becomes of the order of b. The saturation is therefore explained by the breakdown of the two-dimensional nature of the problem. However, for our shear thinning fluids the saturation occurs at values of ρ/b significantly larger than one (figure 4) and depends on the polymer concentration. This suggests that a non-Newtonian property that depends both on the shear rate and concentration of polymers is at the origin of the saturation.

These could, for example, be the stabilization of the shear thinning viscosity on a plateau value for high shear rates or, alternatively, a residual influence of small normal stress effects. The observation that the shear rate at which the saturation occurs decreases with increasing concentration excludes the plateau value of the viscosity as the cause of the saturation, as the stabilization occurs for higher shear rates when the polymer concentration is increased. On the other hand, when increasing the polymer concentration, normal stresses may increase in importance and may also become more pronounced at lower shear rates; these could, in principle, be at the origin of the observed saturation. However, this is in contradiction with the observation that for the solutions of xanthane used here, there are no measurable normal stresses for the shear rates found in the Hele-Shaw cell. We will show in the next section that the normal stresses occur mainly in the thin wetting film left between the glass plates and the finger where the shear rates may be significantly higher than in the rest of the Hele-Shaw cell. The shear rate in the film can be estimated as $\dot{\gamma} \approx U/t$, with t the film thickness from equation (10) below. Taking $U = 10\,\mathrm{cm\,s^{-1}}$, $\mu = 2\,\mathrm{mPa\,s}$, $\sigma = 63\,\mathrm{m\,Nm^{-1}}$ and 0.5 mm for the plate spacing, we find a largest shear rate of $\dot{\gamma} \approx 6900\,\mathrm{s^{-1}}$, not very different from the maximum shear rate in the rheology experiments $\dot{\gamma} \approx 6000\,\mathrm{s^{-1}}$. Therefore, it is also unlikely that residual normal stress effects are at the origin of the saturation. It is also worth noting that, although they may become of importance for the highest speeds (see the calculation of the Reynolds number below), inertial forces cannot be responsible for the observed widening of the fingers as they lead to a narrowing; this is discussed in detail below. Therefore, the observed saturation (and increase) remains to be understood.

Finally, the last inconvenient point of the finger selection discussed above is that it contains one adjustable parameter that has to be determined experimentally: the proportionality constant between α and the shear-thinning exponent n. This means that rheological data alone are not sufficient to predict the finger width. In order to do better, it is possible to solve the (modified) equations (1)–(3) directly for a power-law fluid. This was done by Corvera Poiré & Ben Amar (1998) and Ben Amar & Corvera Poiré (1999) for weakly shear thinning fluids. As it is not clear at which shear-thinning exponent their approximations break down, we can attempt to compare the results for our 'strongly' shear-thinning fluid to their numerical calculations.

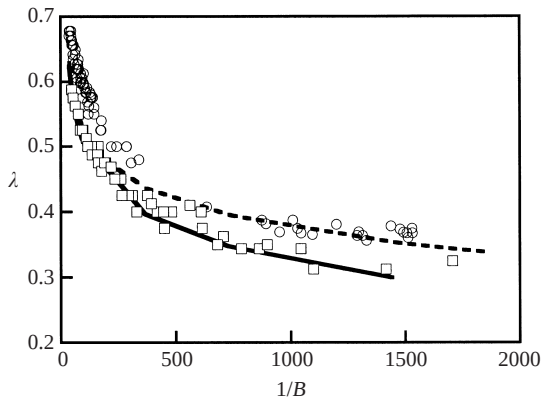

FIGURE 7. Comparison between a direct numerical resolution of equations (1)–(3) for power-law fluids and the experimental data for a ○, 500 w.p.p.m. and □, 1000 w.p.p.m. xanthane solutions.

In (Lindner *et al.* 2000*b*), we compared one data set (for one aspect ratio of the Hele-Shaw cell) in the non-saturated regime to the direct numerical resolution of the equations, and found a reasonable agreement. Figure 7 shows the new and more extensive experimental results for solutions of xanthane of 500 w.p.p.m. ($n = 0.6$) and 1000 w.p.p.m. ($n = 0.46$) obtained for different cell geometries. For both concentrations only the results for the non-saturated regime are shown. For the concentration of 1000 w.p.p.m., these results correspond to the data that fall on the universal curve shown in figure 6; for the comparison made in figure 7, we no longer distinguish different cells using different symbols in the figure. The data for the concentration of 500 w.p.p.m. are obtained in the same way. The experimental data are now compared to the numerical results for the corresponding value of n; a good agreement is obtained, although some deviations are observed for small speeds. These results differ from those reported by Lindner *et al.* (2000*b*) as we focus mainly on the part of the curve before the high-velocity plateau; we left out the comparison at high velocities, since the uncertainty on the numerical values is somewhat larger here.

Furthermore, we can conclude that the numerical results obtained by Corvera Poiré & Ben Amar (1998) and Ben Amar & Corvera Poiré (1999) are in good agreement with the prediction of equation (7) when using the proportionality constant α obtained from the experimental results for the radius of curvature at the finger tip.

5. The effect of normal stresses: the flexible polymer PEO

5.1. *Rheology*

We measure the non-Newtonian viscosity and the first normal stress difference in the range $100\,\mathrm{s}^{-1} < \dot{\gamma} < 6000\,\mathrm{s}^{-1}$ using water as a reference. The measurements are performed on a Reologica StressTech rheometer equipped with a normal force transducer. We use a large cone (55 mm) with a small cone angle (0.5°) in order to measure small normal stress differences at high shear rates (Lindner, Vermant & Bonn 2002).

The results for the viscosity and first normal stress difference N_1 are shown in figures 8 and 9. The normal stress effects are large, both compared to those for the rigid polymers, and compared to the viscous stresses. The viscosity, on the other hand, depends only slightly on the shear rate. This behaviour is best modelled by the Oldroyd-B model (Bird *et al.* 1987), featuring a constant viscosity μ and a quadratic

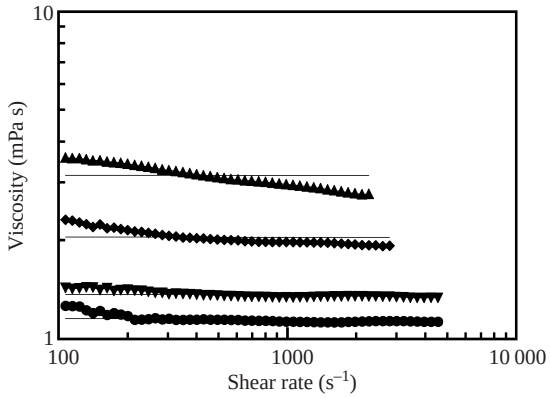

FIGURE 8. Viscosity versus shear rate for solutions of PEO, for concentrations of ●, $c = 125$ w.p.p.m.; ▼, 250 w.p.p.m.; ◆, 500 w.p.p.m.; ▲, 1000 w.p.p.m.

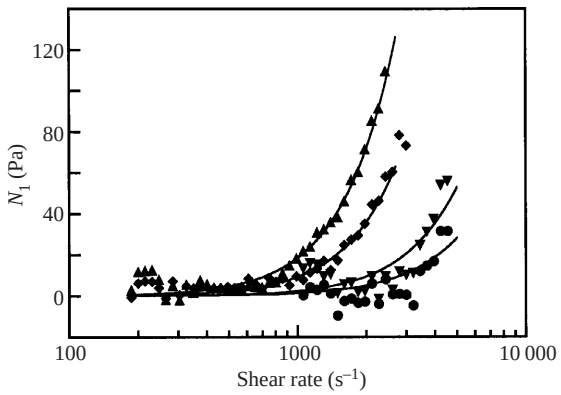

FIGURE 9. First normal stress difference versus shear rate for solutions of PEO, for concentrations of $c = 125$ w.p.p.m., 250 w.p.p.m., 500 w.p.p.m. and 1000 w.p.p.m. (symbols as in figure 8).

first normal stress difference, $N_1 = \Psi_1 \dot{\gamma}^2$, ($\Psi_1$ is the so-called first normal stress coefficient) where:

$$\mu = \mu_s + N k_B T \tau, \tag{8}$$

and

$$\Psi_1 = 2 N k_B T \tau^2, \tag{9}$$

where μ_s is the solvent viscosity, N is the number density of polymer molecules and $k_B T$ the thermal energy. The only adjustable parameter of the model is the relaxation time τ. The fits are shown in the figures and describe the data in a satisfactory way; the values obtained for τ by fitting the rheological data are given in table 1. It is evident from these measurements that the dominant non-Newtonian property of the solutions of PEO are the elastic effects, notably the significant normal stresses. These are due to the stretching of the flexible polymer molecules in the flow field. The same stretching also entails an important resistance to stretching (elongational) motion, or elongational viscosity, that can be orders of magnitude higher than the shear viscosity (Bird *et al.* 1987; Bergeron *et al.* 2000).

	Concentration (w.p.p.m.)	τ (s)
Fit parameters Oldroyd-B fluid PEO (from N_1)	1000	0.00385
	500	0.00383
	250	0.0027
	125	0.0026
Fit parameters Oldroyd-B fluid PEO (from η)	1000	0.00349
	500	0.00339
	250	0.0024
	125	0.00197

TABLE 1. Values of τ obtained by fitting the rheological data.

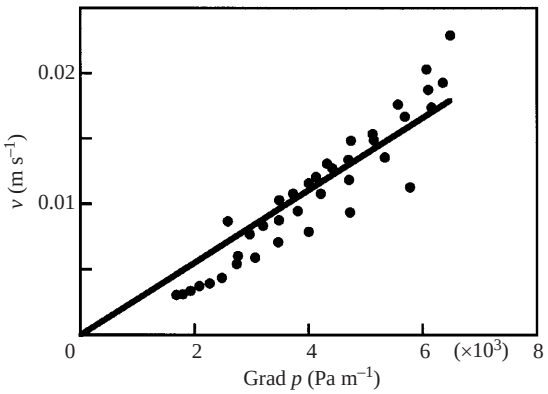

FIGURE 10. Velocity as a function of the applied pressure gradient for a PEO solution of 250 w.p.p.m., together with a linear fit of the data as would follow from Darcy's law with a constant viscosity.

5.2. *Darcy's law*

As the flow near the tip of the viscous fingers is partly elongational, the question arises whether the large elongational viscosity of the PEO solutions possibly intervenes in the fingering instability. This large elongational viscosity gives the large resistance to the stretching flow of these polymer solutions. The flow near the tip of the finger being partly a stretching flow, we might wonder whether this influences the propagation velocity of the finger for a given pressure gradient, which, in turn, could modify the finger width selection.

We therefore study the validity of Darcy's law directly in the fingering experiment for the solutions of PEO. Figure 10 depicts the velocity v as a function of the applied pressure gradient for a PEO solution of 250 w.p.p.m., together with a linear fit of the data as would follow from Darcy's law with a constant viscosity. Despite the fact that there is some scatter in the data owing to the low viscosity of the sample, we conclude that the relation between the velocity and the pressure gradient is linear. This is in agreement with the observation that the shear viscosity of the solutions of PEO is almost a constant. In addition, if we calculate the viscosity from the slope using the Newtonian Darcy's law, equation (1), we obtain $\mu = 1.76 \pm 0.36$ mPa s in agreement with the rheological data for the shear viscosity; the fit using the Oldroyd-B model gives $\mu = 1.43$ mPa s. The study of Darcy's law for this polymer thus demonstrates that the fluid can be taken to have a constant viscosity. Therefore, for the solutions of

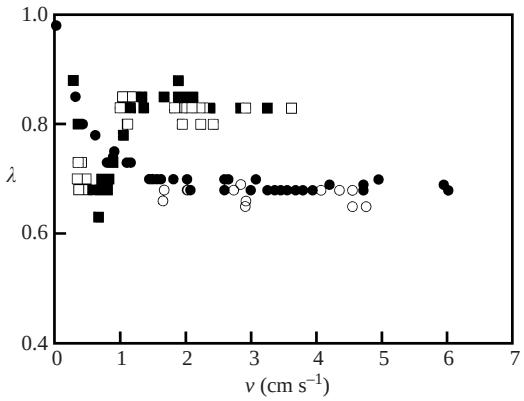

FIGURE 11. Results for λ as a function of the velocity for two different concentrations of PEO. ○, ●, 50 w.p.p.m.; □, ■, 250 w.p.p.m. Filled symbols correspond to viscous fingers, open symbols to finite bubbles in the Hele-Shaw cell.

the flexible polymer PEO, the velocity as a function of the applied pressure gradient is described well by the Newtonian Darcy's law, and we consequently exclude the possibility of an important influence of the very large elongational viscosity on the propagation velocity of the fingers.

5.3. *Finger selection*

Measurements of the finger width for the solutions of PEO have been reported previously (Bonn *et al.* 1995; Bonn & Meunier 1997). As a representative sample from these measurements, the relative finger width λ as a function of the finger velocity U is depicted in figure 11 for two different concentrations: 50 w.p.p.m. and 250 w.p.p.m. Note that it is not possible to obtain data for higher velocities than those shown in figure 11, as no stable fingers are observed for such velocities; tip splitting instabilities are observed for higher speeds. Contrary to the observations for the shear thinning fluid for which a narrowing of the fingers was observed, a widening of the finger compared to the Newtonian case is found (see also snapshot in figure 2*b*). This widening becomes more pronounced as the polymer concentration increases. For a concentration of 50 w.p.p.m., λ decreases with increasing velocity and stabilizes on a plateau with $\lambda > 0.5$ for high velocities. For 250 w.p.p.m., we observe first a decrease, and then an increase followed by a stabilization on a plateau value again with $\lambda > 0.5$, and also higher than the values observed for 50 w.p.p.m. However, the selection mechanism for the finger width was not understood, in spite of several efforts in this direction (Bonn *et al.* 1995; Bonn & Meunier 1997). In the following, we explain the widening of the viscous fingers.

Bonn & Meunier (1997) studied the flow of finite bubbles in a capillary, measuring the thin wetting film left between the moving bubble and the walls of the tube. In the limit of small capillary number, for Newtonian fluids, the thickness t of the film is (Bretherton 1961):

$$\frac{t}{R} = 0.643(3Ca)^{2/3}, \tag{10}$$

where R is the radius of the tube. When polymers were added, they observed film thicknesses much larger than those predicted by (10). The explanation for the increase of the film thickness was that high normal stresses in the film exert an extra pressure on the bubble which becomes more elongated. Bonn & Meunier also suggested that

for the viscous fingers in the Hele-Shaw cell, a similar effect could lead to an extra pressure within the wetting film between the advancing finger and the glass plates of the cell. This extra pressure could cause a change in the finger width and could thus be responsible for the observed finger widening in the PEO solutions. We will examine this proposition here.

In order to do this, it is necessary to recall that in the bubble experiment, the normal stresses responsible for the film thickening result from the high shear rate in the film. The existence of such a high shear rate in the film left between the viscous finger and the glass plates is less obvious as the rear of the finger does not move. As a first experiment, we therefore study finite bubbles in the Hele-Shaw cell. We used two different polymer concentrations: 50 w.p.p.m. and 250 w.p.p.m.; we again measure the width of the bubble as a function of its velocity. In these experiments, the length of the bubble was always several times higher than its width. The results are compared to those for the fingers in figure 11, from which we can conclude that the width of the bubbles is indistinguishable from that of the fingers. This shows that either for the fingers, high normal stresses may also develop in the wetting film, or the polymers act in the same way at the tip of the bubbles and the fingers, leading to the observed widening. The stresses in the wetting film adapt themselves to what happens at the tip. This observation allows us thus to calculate the shear rate that occurs in the wetting film of the fingers in the same way as for the bubbles.

We subsequently performed interferometric measurements of the wetting film thickness (Tabeling & Libchaber 1986). We find that Bretherton's law remains valid to within the experimental error (replacing the radius R by the plate spacing b in equation (10)) for all concentrations that we tested (up to 1000 w.p.p.m.). The film thickness for the solutions of PEO is very close to the thickness obtained for Newtonian fluids (data not shown). This result is very different from the large increase of the film thickness observed for air bubbles in a circular tube. This is logical, in fact, as for the fingers it is much easier to deform in the direction of the finger width, as the radius of curvature is much larger there, than in the direction perpendicular to the glass plates. We could therefore anticipate a widening of the fingers rather than a significant thickening of the film, exactly as is observed in the experiments. In order to see whether an extra pressure on the finger because of the normal stresses can quantitatively account for the observations, we first discuss the results for the relative finger width as a function of the control parameter $1/B = 12Ca(W/b)^2$. New results for $b = 0.5$ mm, $W = 4$ cm and 5, 50 and 500 w.p.p.m. PEO solutions, are shown in figure 12, together with the universal curve for Newtonian fluids. It can be seen that the results for the different concentrations do not coincide with the universal curve of McLean & Saffman (1981). Note that we observe a destabilization of the fingers at values of $1/B$ as low as 200. For Newtonian fingers it is known that the destabilization of the fingers occurs at significantly higher values of $1/B$ (Park & Homsy 1986). Observations of the destabilization at low values of $1/B$ for fingers in solutions of PEO have been made before and were interpreted as being due to normal stress effects (Vlad & Maher 1993).

We subsequently include the extra pressure that the normal stresses exert on the finger in the control parameter $1/B$. To do so, we calculate the normal stress difference N_1 that occurs in the thin wetting film using the Oldroyd-B model (equation (9)). Furthermore, as in Bonn & Meunier (1997), we assume a no-slip boundary condition at the air–polymer solution interface. Then, in the film, the shear rate $\dot{\gamma} \approx U/t$ where t is the film thickness calculated from Bretherton's law. We therefore suppose that $\dot{\gamma} = \beta(U/t)$ where β is a constant of order unity. The normal stress difference exerts

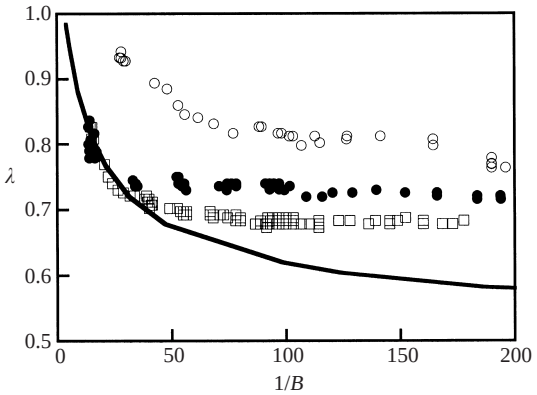

FIGURE 12. Results for λ as a function of the control parameter for □, $c = 5$ w.p.p.m. ●, 50 w.p.p.m.; ○, 500 w.p.p.m., of PEO for a channel width of $W = 4$ cm and $b = 0.5$ mm. The drawn line is the McLean–Saffman result for Newtonian fluids.

an extra pressure on the finger that has to be added to the capillary pressure in the direction of the plate spacing. The pressure jump at the interface then reads

$$\Delta p = \sigma\kappa + \frac{2\sigma}{b} + N_1(\dot{\gamma}), \tag{11}$$

where κ is the curvature in the direction of the channel width. Note that the radius of curvature in the direction of the plate spacing is taken to be $\frac{1}{2}b$, as in Saffman & Taylor (1958). This allows us to define an effective surface tension, which includes N_1, in a similar way to Tabeling & Libchaber (1986) for the Newtonian case. Neglecting the (small) first term on the right-hand side, the effective surface tension $\sigma_{eff} = \sigma + \frac{1}{2}N_1(\dot{\gamma})b$ leads to a corrected control parameter:

$$\frac{1}{B_{corr}} = 12\frac{\mu U}{\sigma + \frac{1}{2}N_1(\dot{\gamma})b}\left(\frac{W}{b}\right)^2. \tag{12}$$

When plotting the relative width of the viscous fingers for $c = 5$, 50 and 500 w.p.p.m. PEO as a function of this new control parameter (figure 13), we observe that the data collapse onto a single universal curve. Equation (12) defines the 'real' control parameter for our problem. As for the precise value of the proportionality constant between $\dot{\gamma}$ and U/t, we find that $\beta = 2.8$ gives the best rescaling of the data. This means that U/t is indeed the correct order of magnitude for the shear rate, but that it gives an estimate that is slightly too low. This could in part be due to the fact that there are small deviations from the film thickness predicted by Bretherton's law (equation (10)), which was obtained by Bretherton (1961) as an expansion for small velocities (small capillary numbers). For non-Newtonian fluids having normal stress effects (Oldroyd-B fluids), smaller film thicknesses were indeed predicted theoretically by Ro & Homsy (1995), as discussed below. In addition, even for the Newtonian case, equation (10) gives an estimate for the maximum film thickness corresponding to the lowest shear rate; therefore, a somewhat higher average shear rates is necessary to rescale the data.

Moreover, the universal curve that is found is, in fact, in good agreement with the classical results of McLean & Saffman (1981) for values of $1/B_{corr}$ that are not too high. For higher values, the results deviate from the universal curve. The data seem to stabilize on a plateau value higher than the classical value $\lambda = 0.5$.

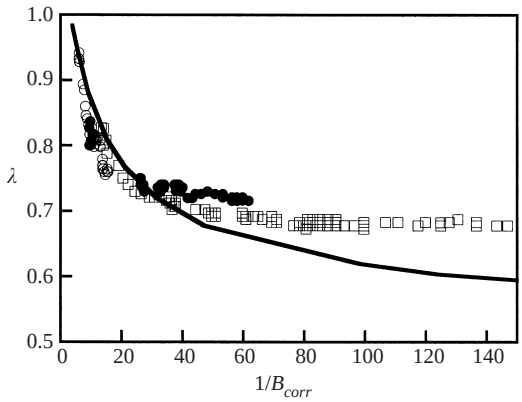

FIGURE 13. Same data as in figure 12, but now plotted as a function of the corrected control parameter that takes normal stress effects into account.

Two explanations are possible for this observation. First, at the highest speeds, inertial effects may come into play. If we define the Reynolds number with the plate spacing as the relevant length scale, we have $Re \approx \rho U b/\mu$, ($\rho \approx 10^3\,\mathrm{kg\,m^{-3}}$ being the liquid density) which can become of order unity for the highest speeds considered here. Gondret & Rabaud (1997) recently formulated an approximate way to include inertial effects in Hele-Shaw flow, averaging over the small gap. Using this approximation, Ben Amar & Bonn (2002) were able to estimate the effects of inertia on the width of (Newtonian) viscous fingers. Relative to the McLean–Saffman result, they find fingers that either have the same width, or are narrower. Therefore, inertial effects cannot account for the observation that the fingers are wider than expected. The second option to account for the widening is that the observed plateau is due to the presence of impurities in the cell. It turns out to be very difficult to make the glass plates perfectly wetting to pure water; in the experiments, a pinning of the interface at wetting defects is often observed using pure water. For such anomalous fingers, we observe a stabilization around $\lambda \approx 0.7$ for the values of the control parameter considered here. These values are similar to those observed for PEO at high speeds, and thus could provide an alternative explanation. It should be noted that with PEO, however, the pinning of the interfaces is observed less frequently, probably because the polymer changes the wettability a little. For xanthane, the pinning is never observed and the finger width stabilizes at $\lambda \approx 0.5$ for high speeds in the limit of low polymer concentration. The latter observation gives us some confidence that the deviation from the McLean–Saffman result is likely to be an experimental effect due to wetting defects on the glass plates.

In conclusion, the corrected control parameter that includes the normal stress allows us to rescale the experimental data for different PEO concentrations. For low $1/B_{corr}$, the universal curve is in good agreement with the classical result of McLean & Saffman. For higher values of $1/B_{corr}$, we find a small deviation from the classical results. This deviation is likely to be due to an experimental effect, but cannot be explained quantitatively for the moment.

Finally, the observed increase in finger width with increasing velocity that is sometimes observed (figure 11) remains unaccounted for. Although it can, in principle, be envisaged that the competition between capillary, viscous and elastic forces leads to such behaviour, for the parameters used here, an increase of λ with the velocity is never observed.

Comparing with theory, Ro & Homsy (1995) analysed the thickness of the film in the Saffman–Taylor problem for an Oldroyd-B fluid. We have shown above that the solutions of PEO we use are described well by this model. Ro & Homsy predict a slight decrease of the film thickness compared to Newtonian fluids for the elastic fluid, not in contradiction with our findings. However, it should be noted that their results are valid for both small capillary and Weissenberg numbers, We. The Weissenberg number is a measure of the importance of the elastic effects of the fluid and can be defined as the ratio of the relaxation time of the polymers and a characteristic time of the flow, given by $1/\dot{\gamma}$. For a typical relaxation time $\tau = 3\,\mathrm{ms}$ (typical for concentrations smaller than 500 w.p.p.m.) and a typical shear rate observed in the viscous fingering experiment we obtain $We \approx 1$, which can hardly be considered as small. Wilson (1990), in another theoretical paper, considered the basic equations for the stability of the interface, also employing the Oldroyd-B model, but did not come up with explicit predictions for the finger width in steady state. As far as we know, no other theory exists on this problem.

6. Summary and conclusions

We have considered the Saffman–Taylor or viscous fingering instability in two different polymer solutions, each exhibiting in essence only a single non-Newtonian flow property. Solutions of rigid polymers show a strong shear-thinning behaviour, but have negligible elastic effects. Flexible polymer solutions, on the other hand, show negligible shear thinning but strong elastic effects, notably normal stresses that can easily exceed the viscous stresses and a large elongational viscosity. Investigation of the fingering instability for these polymer solutions allows us to consider the effect of the most common non-Newtonian effects on the fingering instability separately.

For the shear-thinning polymer solutions, we have shown that the results for the relative finger width as a function of the finger velocity separate into two different regimes. For low polymer concentrations, the non-Newtonian effects are weak. They can be taken into account solely by taking the shear-thinning viscosity into account both in an effective Darcy's law, and in the control parameter. If this is done, results obtained for different concentrations, different dimensions of the Hele-Shaw cell all scale onto the universal curve for Newtonian fluids.

For higher polymer concentrations, the shear-thinning effects become more important. This not only leads to a modification of Darcy's law but also the fingers become narrower than is possible for the Newtonian case ($\lambda < 0.5$) so that automatically there is no hope of rescaling onto the Newtonian result. We show that it is the radius of curvature at the tip that is selected. Once this is admitted, two roads to a quantitative understanding of the instability are open. The first one is to relate the shear-thinning behaviour phenomenologically to the dependence of the radius of curvature ρ on the capillary number. Here, we find a linear relationship between the shear-thinning exponent and the slope of ρ vs. $1/\sqrt{Ca}$. This allows us to define a new universal curve for a given shear-thinning fluid. Results for different cell dimensions are shown to collapse onto this universal curve. The second possibility to quantitatively account for the data is to solve the governing equations numerically. This also leads to a fair agreement between theory and experiment.

For the elastic polymer solutions, under similar conditions, much wider fingers are found than for Newtonian fluids, in contrast with the narrower fingers observed for the shear-thinning polymer. A study of Darcy's law allows for the conclusion that the

influence of the high elongational viscosity of such polymer solutions typically does not show up in the propagation velocity of the fingers. The other important elastic effects are the large normal stresses such solutions exhibit. We show that these can be taken into account in the pressure drop over the interface, and they can consequently be incorporated in an effective surface tension. If this tension is incorporated in the control parameter a satisfactory data collapse occurs. Moreover, the data almost coincide with the universal curve for Newtonian fluids.

In conclusion, we have succeeded in understanding the relation between the rheological properties of a given non-Newtonian fluid and the fingering instability occurring in these fluids. This should be helpful in understanding what happens in more complex fluids such as foams, clay pastes, slurries, polymer melts and gels encountered in numerous applications as oil recovery, hydrology or injection moulding, for which fingering instabilities may be relevant.

We are indebted to Yves Couder for helpful discussions. The Laboratoire de Physique Statistique of the Ecole Normale Supérieure is UMR 8550 of the CNRS, associated with the universities Paris 6 and Paris 7. A. L. has benefited from a scholarship from the DAAD under program HSP III.

REFERENCES

Ben Amar, M. 1995 Viscous fingering: a singularity in Laplacian growth models. *Phys. Rev.* E **51**, R3819–R3822.

Ben Amar, M. & Bonn, D. 2002 The effect of inertia on viscous fingering in a Hele-Shaw cell. In preparation.

Ben Amar, M. & Corvera Poiré, E. 1999 Pushing a non-Newtonian fluid in a Hele-Shaw cell: from fingers to needles. *Phys. Fluids* **11**, 1757–1767.

Bensimon, D., Kadanoff, L. P., Liang, S., Shraiman, B. I. & Tang, C. 1986 Viscous flows in two dimensions. *Rev. Mod. Phys.* **58**, 977–999.

Bergeron, V., Bonn, D., Martin, J.-Y. & Vovelle, L. 2000 Impact and retraction of viscoelastic drops. *Nature* **405**, 772.

Bird, R. B., Armstrong, R. C. & Hassager, O. 1987 *Dynamics of Polymeric Liquids*. Wiley.

Bonn, D., Kellay, H., Ben Amar, M. & Meunier, J. 1995 Viscous finger widening with surfactants and polymers. *Phys. Rev. Lett.* **75**, 2132–2135.

Bonn, D., Kellay, H. & Meunier, J. 1998 Viscous fingering and related instabilities in complex fluids. *Phil. Mag.* B **78**, 131–142.

Bonn, D. & Meunier, J. 1997 Viscoelastic free boundary problems: non-Newtonian viscosity *vs.* normal stress effects. *Phys. Rev. Lett.* **79**, 2662–2665.

Bretherton, F. P. 1961 The motion of long air bubbles in tubes. *J. Fluid Mech.* **10**, 166–188.

Combescot, R., Dombre, T., Hakim, V., Pomeau, Y. & Pumir, A. 1986 Shape selection of Saffman–Taylor fingers. *Phys. Rev. Lett.* **56**, 2036–2039.

Corvera Poiré, E. & Ben Amar, M. 1998 Finger behavior of a shear thinning fluid in a Hele-Shaw cell. *Phys. Rev. Lett.* **81**, 2048–2051.

Couder, Y. 1991 Growth patterns: from stable curved fronts to fractal structures. In *Chaos, Order and Patterns* (ed. R. Artuso, P. Cvitanovic & G. Casati). Plenum.

Couder, Y., Gerard, N. & Rabaud, M. 1986 Narrow fingers in the Saffman–Taylor instability. *Phys. Rev.* A **34**, 5175–5178.

Daccord, G., Nittmann, J. & Stanley, H. E. 1986 Radial viscous fingers and diffusion limited aggregation: fractal dimensions and growth sites. *Phys. Rev. Lett.* **56**, 336–339.

van Damme, H., Alsac, E., Laroche, C. & Gatineau, L. 1988 On the respective roles of low surface tension and non-Newtonian rheological properties in fractal fingering. *Europhys. Lett.* **5**, 25–30.

Fast, P., Kondic, L., Shelley, M. J. & Palffy-Muhoray, P. 2001 Pattern formation in non-Newtonian Hele-Shaw flow. *Phys. Fluids* **13**, 1191–1212.

Gondret, P. & Rabaud, M. 1997 Shear instability of two-fluid parallel flow in a Hele-Shaw cell. *Phys. Fluids* **9**, 3267–3274.

Homsy, G. M. 1987 Viscous fingering in porous media. *Ann. Rev. Fluid Mech.* **19**, 271–311.

Hong, D. C. & Langer, J. S. 1986 Analytic theory of the selection mechanism in the Saffman–Taylor problem. *Phys. Rev. Lett.* **56**, 2032–2035.

Kawaguchi, M., Shibata, A., Shimoto, K. & Kato, T. 1998 Effect of geometry and anisotropy of a Hele-Shaw cell on viscous fingering of polymer solutions. *Phys. Rev.* E **58**, 785–788.

Kessler, D. A. & Levine, H. 1985 Stability of finger patterns in Hele-Shaw cells. *Phys. Rev.* A **32**, 1930–1933.

Kondic, L., Palffy-Muhoray, P. & Shelley, M. J. 1996 Models of non-Newtonian Hele-Shaw flow. *Phys. Rev.* E **54**, R4536–R4539.

Kondic, L., Shelley, M. J. & Palffy-Muhoray, P. 1998 Non-Newtonian Hele-Shaw flow and the Saffman–Taylor instability. *Phys. Rev. Lett.* **80**, 1433–1436.

Lemaire, E., Levitz, P., Daccord, G. & van Damme, H. 1991 From viscous fingering to viscoelastic fracturing in colloidal fluids. *Phys. Rev. Lett.* **67**, 2009–2012.

Lindner, A., Bonn, D. & Meunier, J. 2000*b* Viscous fingering in a shear thinning fluid. *Phys. Fluids* **12**, 256–261.

Lindner, A., Coussot, P. & Bonn, D. 2000*a* Viscous fingering in a yield stress fluid. *Phys. Rev. Lett.* **85**, 314–317.

Lindner, A., Vermant, J. & Bonn, D. 2002 How to obtain the elongational viscosity of dilute polymer solutions? *Physica* A (in press).

McCloud, K. V. & Maher, J. V. 1995 Experimental perturbations to Saffman–Taylor flow. *Phys. Rep.* **260**, 139–185.

McLean, J. W. & Saffman, P. G. 1981 The effect of surface tension on the shape of fingers in a Hele-Shaw cell. *J. Fluid Mech.* **102**, 455–469.

Park, S. S. & Durian, D. J. 1994 Viscous and elastic fingering instabilities in foam. *Phys. Rev. Lett.* **72**, 3347–3350.

Park, C.-W. & Homsy, G. M. 1986 The instability of long fingers in Hele-Shaw flows. *Phys. Fluids* **28**, 1583–1585.

Park, C.-W. & Homsy, G. M. 1984 Two-phase displacement in Hele-Shaw cells: theory. *J. Fluid Mech.* **139**, 291–308.

Rabaud, M., Couder, Y. & Gerard, N. 1988 Dynamics and stability of anomalous Saffman–Taylor fingers. *Phys. Rev.* A **37**, 935–947.

Reinelt, D. A. & Saffman, P. G. 1985 The penetration of a finger into a viscous fluid in a channel and tube. *SIAM* **6**, 542–561.

del Río, J. A., López de Haro, M. & Whitaker, S. 1998 Enhancement in the dynamic response of a viscoelastic fluid flowing in a tube. *Phys. Rev.* E **58**, 6323–6327.

Ro, J. S. & Homsy, G. M. 1995 Viscoelastic free surface flows: thin film hydrodynamics of Hele-Shaw and dip coating flows. *J. Non-Newtonian Fluid Mech.* **57**, 203–225.

Sader, J. E., Chan, D. Y. C. & Hughes, B. D. 1994 Non-Newtonian effects on immiscible viscous fingering in a radial Hele-Shaw cell. *Phys. Rev.* E **49**, 420–432.

Saffman, P. G. & Taylor, G. I. 1958 The penetration of a fluid into a porous medium or Hele-Shaw cell containing a more viscous liquid. *Proc. R. Soc. Lond.* A **245**, 312–329.

Shaw, B. E. 1980 Universality in selection with local perturbations in the Saffman–Taylor problem. *Phys. Rev.* A **40**, 5875–5895.

Shraiman, B. I. 1986 Velocity selection and the Saffman–Taylor problem. *Phys. Rev. Lett.* **56**, 2028–2031.

Smith, D. E., Wu, X. Z., Libchaber, A., Moses, E. & Witten, T. 1992 Viscous finger narrowing at the coil-stretch transition in a dilute polymer solution. *Phys. Rev.* A **45**, R2165–R2168.

Tabeling, P. & Libchaber, A. 1986 Film draining and the Saffman–Taylor problem. *Phys. Rev.* A **33**, 794–796.

Vlad, D. H. & Maher, J. V. 1993 Tip splitting instabilities in the channel flow of constant viscosity elastic fluids. *Phys. Rev.* E **61**, 5439–5444.

Wilson, S. D. R. 1990 The Taylor–Saffman problem for a non-Newtonian liquid. *J. Fluid Mech.* **220**, 413–425.

Zhao, H. & Maher, J. V. 1993 Associating-polymer effects in a Hele-Shaw experiment. *Phys. Rev.* E **47**, 4278–4283.

Zocchi, G., Shaw, B. E., Libchaber, A. & Kadanoff, L. P. 1987 Finger narrowing under local perturbations in the Saffman–Taylor instability. *Phys. Rev.* A **36**, 1894–1900.